

Application of GUF for a multi-output iterative measurement model estimation according to GUM S2 in indirect five-axis CNC machine tool calibration

A. Los, J. R. R. Mayer

Department of Mechanical Engineering, Polytechnique Montreal, QC, Canada

Abstract

The paper looks at the problem of estimating the uncertainty of the five-axis machine tool indirect calibration method, using (generalized) GUM Uncertainty Framework (GUF) presented in Guide to the Expression of Uncertainty in Measurement Supplement 2 (GUM S2). The analysed Scale Enriched Master Balls Artefact (SAMBA) probing calibration method is solved through an iterative calculation (for each iteration the calculation model changes and depends on the previous one), which causes difficulties when the measurement model sensitivity matrix has to be defined analytically. That is why a numerical Jacobian is used. The simulated results of the machine geometric errors uncertainties estimation are presented for different number and configuration of master balls used in the SAMBA artefact.

1 Introduction

Calibration of multi-axis machine tools requires estimating their geometric errors parameters. This can be achieved through direct or indirect methods [1]. The former involve measuring each parameter separately using, for example, laser interferometry. The latter allow estimating a number of those parameters from the measurement of volumetric effects within the machine workspace. The devices used for indirect calibration are, among others, ‘chase-the-ball’ [2], SAMBA [3], self-tracking laser interferometers etc.

Calibration results can be evaluated through different means. Bringmann *et al.* [4] compare different calibration strategies through the uncertainty on the workpiece feature errors estimated from the calibration results

using the Monte Carlo method (MCM). In [2] the calibration results are evaluated through their uncertainty obtained from the MCM simulation of the full machine model. Schwenke *et al.* [5] estimate the machine parametric errors from the interferometric displacement measurements. In order to calculate the calibration results uncertainty, the MCM simulations are performed with the randomly distributed noise added to the measurement results. The standard deviations of the parameters represent their standard uncertainties and are used for optimizing the measurement strategy.

Because the indirect calibration methods have a multi-output model, their uncertainty evaluation should be estimated following the GUM S2 [6] rather than the GUM [7]. In this study, the (generalized) GUM uncertainty framework is applied for the uncertainty calculation of the SAMBA method, which has a multi-output model and an iterative solution.

2 SAMBA

The SAMBA calibration method [3] requires probing the artefact consisting of a number of master balls and a scale bar in different machine rotary axis indexations. In Figure 1 (left) the artefact with 4 master balls (with a diameter of 12.7 mm) and the scale bar (with a length of 304.6686 mm) mounted on the table of the Mitsui Seiki five-axis machine tool is shown. The kinematic model of the machine is depicted in Figure 1 (right). During the SAMBA measurements, the balls are probed in five points which allows calculating their centre position coordinates.

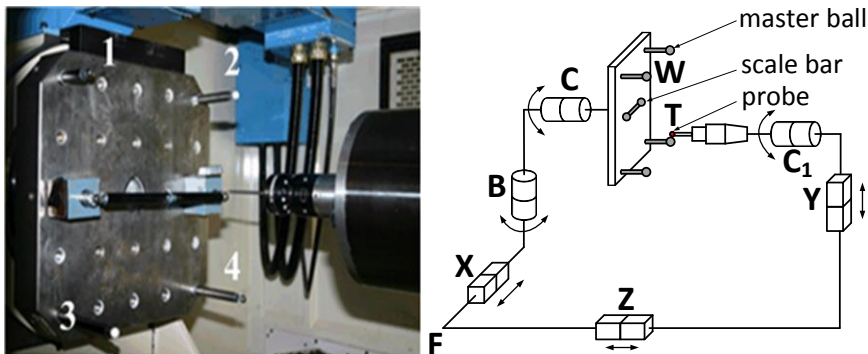


Figure 1: left: SAMBA artefact probed on the machine tool for $[b, c]=[0, 0]$;
 right: five-axis machine tool kinematic model with the topology WCBXFZ C_1 T; W - workpiece, T - tool, F - machine foundation, B, C – rotary axes around the Y and Z axes respectively, X, Y, Z – machine linear axes, C_1 – spindle.

Figure 2 shows the SAMBA method algorithm for identifying the m output quantities Y with the estimate $y=(y_1, \dots, y_m)$ from the N input quantities X with the

estimate $\mathbf{x}=(x_1, y_1, z_1, \dots, x_{(N-1)/3}, y_{(N-1)/3}, z_{(N-1)/3}, L)$, where x, y, z are the measured balls centers coordinates and L is the calibrated scale bar length.

In order to identify the geometric errors parameters the machine kinematic model needs to be built [8]. That allows predicting the tool position (virtual tool position at the ball centre) and comparing it with the measured ball centre position by using the homogenous transformation matrix (HTM) ${}^{ball}T_{tip}$, which results in calculating the residual volumetric error \mathbf{x}_R . In order to reduce this error, the Newton-Gauss approach is applied. The machine sensitivity Jacobian matrix \mathbf{J} is used for calculating the adjustment in machine parameters $\delta\mathbf{y}$ from the equation:

$$\mathbf{x}_R + \mathbf{J} \cdot \delta\mathbf{y} = 0 \quad (1)$$

The calculations are continued until δy_i is smaller than the set threshold value τ .

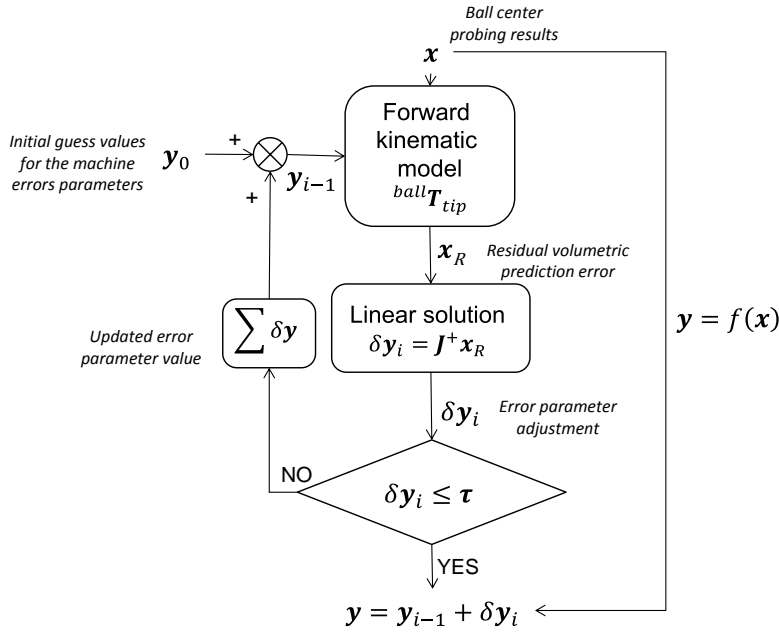


Figure 2: SAMBA flow chart

3 Uncertainty estimation

Since the analysed calibration model is a multi-output model, the uncertainty is estimated according to GUM S2 [6]. The uncertainty is calculated for all the parameters simultaneously. The correlation between the parameters is also

calculated. In order to obtain the uncertainty at the required confidence level p the coverage factor is estimated.

3.1 GUM Uncertainty Framework (GUF)

The GUF method presented in GUM S2 [6] allows estimating the output quantities covariance matrix U_y from the equation:

$$U_y = C_x U_x C_x^T \quad (2)$$

where:

C_x is the sensitivity measurement matrix,

$$C_x = \begin{bmatrix} \frac{\partial f_1}{\partial x_1} & \frac{\partial f_1}{\partial x_2} & \dots & \frac{\partial f_1}{\partial x_N} \\ \frac{\partial f_2}{\partial x_1} & \frac{\partial f_2}{\partial x_2} & \dots & \frac{\partial f_2}{\partial x_N} \\ \vdots & \vdots & \ddots & \vdots \\ \frac{\partial f_m}{\partial x_1} & \frac{\partial f_m}{\partial x_2} & \dots & \frac{\partial f_m}{\partial x_N} \end{bmatrix} \quad (3)$$

U_x is the input data covariance (uncertainty) matrix,

$$U_x = \begin{bmatrix} u(x_1, x_1) & \dots & u(x_1, x_N) \\ \vdots & \ddots & \vdots \\ u(x_N, x_1) & \dots & u(x_N, x_N) \end{bmatrix} \quad (4)$$

where each element (i,j) is

$$u(x_i, x_j) = r(x_i, x_j)u(x_i)u(x_j) \quad (5)$$

with $r(x_i, x_j)$ the correlation coefficient associated with x_i and x_j .

3.2 Numerical Jacobian

Due to the iterative character of the identification procedure the function $y=f(x)$ cannot be expressed analytically. Nevertheless, its sensitive matrix can be estimated as the $N \times m$ numerical Jacobian:

$$C_x \approx J_{num} \quad (6)$$

Each element (n, k) in J_{num} equals:

$$J_{num(n,k)} = \frac{\partial f_k}{\partial x_n} = \frac{f_k(x_1, \dots, x_n + \Delta x_n, \dots, x_N) - f_k(x_1, \dots, x_N)}{\Delta x_n} \quad (7)$$

Adding the Δx_n to each of the N input quantities consecutively allows building the numerical Jacobian column by column.

4 Measurements and simulation

The uncertainty calculation is performed using MATLAB[®]. The simulation is ran in order to calculate the numerical Jacobian and calculate the uncertainty. However, the input data covariance U_x is estimated from 44 repeated SAMBA measurements performed over a 24 hour period. It assures that the correlation between the input data is considered. It also includes any changes in the measurands over that period.

The SAMBA calibration method is performed for the thirteen geometric error parameters listed in

Table 1 with the values obtained during the previous calibration [3]. The measurement is simulated for the seven different rotary axis indexation pairs: $[b, c] = [90, 270], [60, 180], [30, 90], [0, 0], [-90, -270], [-60, -180]$ and $[-30, -90]$ deg. The obtained values allow identifying the calibration results using different number and configuration of master balls. The uncertainty for one master ball used in the artifact is estimated for each of the four balls. When two balls are used it is obtained for all of the six combinations of the balls: 1 and 2; 1 and 3; ... ; 3 and 4. The same for the four configurations of the three balls: 1, 2 and 3; 1,2 and 4; 1, 3 and 4; 2,3 and 4.

Table 1: Identified machine geometric errors parameters [3].

Symbol	Description	Calibration result
E_{AOB}	out-of-squareness of the B-axis relative to the Z-axis (μrad)	0.9
E_{COB}	out-of-squareness of the B-axis relative to the X-axis (μrad)	-1.5
E_{XOC}	distance between the B and C axes (μm)	-102.2
E_{AOC}	out-of-squareness of the C-axis relative to the B-axis (μrad)	3.9
E_{BOC}	out-of-squareness of the C-axis relative to the X-axis (μrad)	19.9
E_{BOZ}	out-of-squareness of the Z-axis relative to the X-axis (μrad)	-37.5
E_{AOY}	out-of-squareness of the Y-axis relative to the Z-axis (μrad)	-8.8
E_{COY}	out-of-squareness of the Y-axis relative to the X-axis (μrad)	23.9
E_{XOCI}	X offset of the spindle relative to the B-axis (μm)	-97.1
E_{YOCI}	Y offset to the spindle relative to the C-axis (μm)	15.7
E_{XX}	positioning linear error term of the X-axis ($\mu\text{m}/\text{m}$)	-45.2
E_{YY}	positioning linear error term of the Y-axis ($\mu\text{m}/\text{m}$)	5.3
E_{ZZ}	positioning linear error term of the Z-axis ($\mu\text{m}/\text{m}$)	-20.5

5 Results

The maximum and minimum parameter uncertainty values obtained for different number and combinations of master balls are depicted in Figure 3. The configuration ball numbers corresponding to the uncertainties are not shown due to the graph clarity but will be introduced in the discussion. All the uncertainties are calculated for the rectangular coverage regions for the coverage probability $p=0.95$, so, depending on the master balls used, the coverage factor varies from 2.9 to 3.0.

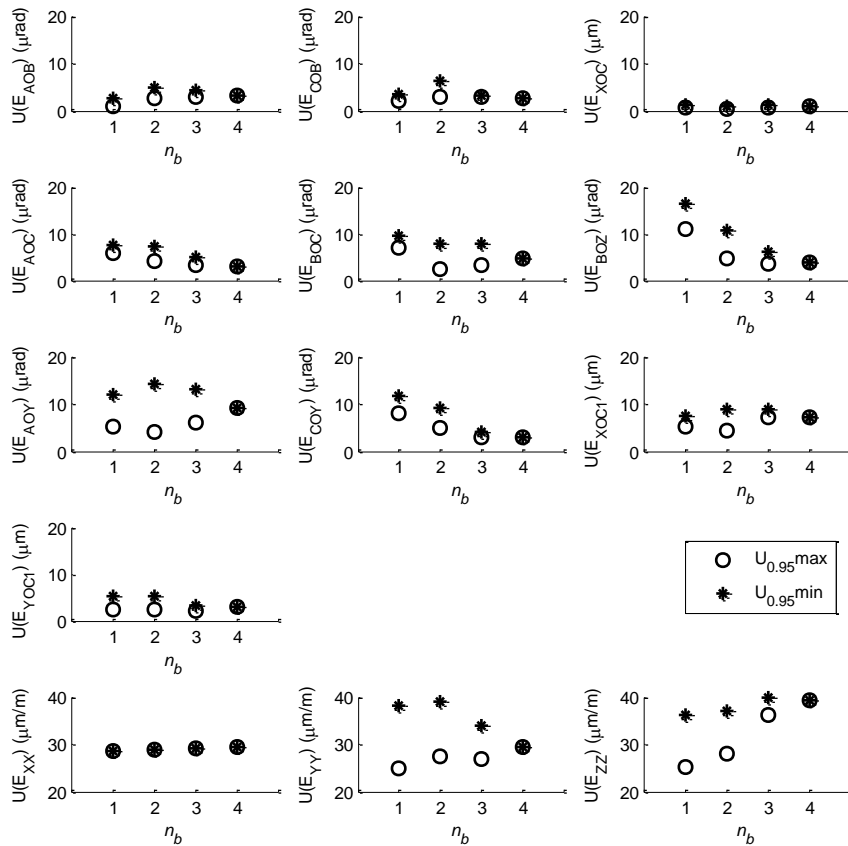


Figure 3: Uncertainty values for different numbers and configurations of SAMBA artefact for the confidence level $p=0.95$.

No clear trend in the influence of the number or combination of master balls on the uncertainty value can be observed for the E_{XX} . This parameter is estimated only from the length of the scale bar L and the measurement of the scale bar balls, so that it cannot be influenced by measurement of the master balls 1, 2, 3, 4. Almost negligible difference for the uncertainty is also observed for the E_{XOC} .

The biggest impact of the number and configuration of the master balls can be observed for the scale errors E_{YY} and E_{ZZ} . In both cases, a larger number of the master balls reduces the uncertainty range and, when one ball is used, the

smallest uncertainty value is obtained for the balls 3 and 4 and the largest for the ball number 1. For the E_{ZZ} the $U_{0.95min}$ and $U_{0.95max}$ values are increasing when more balls are added and the $U_{0.95max}(E_{ZZ})$ for 1 and 2 balls is close to the $U_{0.95min}(E_{ZZ})$ for 3 balls.

The range and the mean values of $U_{0.95}$ are decreasing significantly for the E_{AOC} , E_{BOZ} , E_{COY} , E_{YOC1} when more master balls, larger n_b , are used in the artefact. On the contrary $U(E_{AOB})$ increases with the larger n_b . However, this gain is not as significant as the decrease of the uncertainty of other parameters for higher values of n_b .

6 Conclusion

A method for the uncertainty estimation of the multi-output calibration method has been proposed. The calculation of numerical Jacobian allowed estimating the model sensitivity matrix without defining the analytical equation of the model. This method has a relatively short computation time, compared to the Monte Carlo method, and allows giving the uncertainty result within few minutes although the number of the input and output variables is large.

The uncertainty estimation performed for different SAMBA configurations allowed comparing them and verifying if it is always necessary to use more balls, since measurement takes valuable machining time. The results showed that the uncertainty depends on the number and combination of the balls used. Since there is no best set or a ball that would give the lowest uncertainty for all the parameters, the number of balls should be chosen as the smallest number of the master balls used that gives the results with the uncertainty not lower than the demanded one. With this method the results within the desired uncertainty can be obtained for the shortest possible calibration time.

The artefact with two master balls requires half of the measuring time comparing to the one with four balls. Moreover, the uncertainty for two balls (for most of the parameters) is not significantly lower than for the four balls. Taking those factors into consideration, calibration using SAMBA with two master balls gives satisfactory results.

7 Acknowledgment

This research was supported by the NSERC Canadian Network for Research and Innovation in Machining Technology (NSERC CANRIMT; www.nserc-canrimt.org)

8 References

- [1] H. Schwenke, W. Knapp, H. Haitjema, A. Weckenmann, R. Schmitt, and F. Delbressine, "Geometric error measurement and compensation of machines-An update," *CIRP Annals - Manufacturing Technology*, vol. 57, pp. 660-675, 2008.
- [2] B. Bringmann and W. Knapp, "Model-based 'Chase-the-Ball' Calibration of a 5-Axes Machining Center," *CIRP Annals - Manufacturing Technology*, vol. 55, pp. 531-534, 2006.
- [3] J. R. R. Mayer, "Five-axis machine tool calibration by probing a scale enriched reconfigurable uncalibrated master balls artefact," *CIRP Annals - Manufacturing Technology*, vol. 61, pp. 515-518, 2012.
- [4] B. Bringmann, J. P. Besuchet, and L. Rohr, "Systematic evaluation of calibration methods," *CIRP Annals - Manufacturing Technology*, vol. 57, pp. 529-532, 2008.
- [5] H. Schwenke, M. Franke, J. Hannaford, and H. Kunzmann, "Error mapping of CMMs and machine tools by a single tracking interferometer," *CIRP Annals - Manufacturing Technology*, vol. 54, pp. 475-478, 2005.
- [6] GUM, "Evaluation of measurement data – Supplement 2 to the "Guide to the expression of uncertainty in measurement" – Extension to any number of input quantities," ed, Joint Committee for Guides in Metrology, JCGM 102:2011.
- [7] GUM, "Evaluation of measurement data - Guide to the expression of uncertainty in measurement," ed, Joint Committee for Guides in Metrology, JCGM 100:2008.
- [8] Y. A. Mir, J. R. R. Mayer, and C. Fortin, "Tool path error prediction of a five-axis machine tool with geometric errors," *Proceedings of the Institution of Mechanical Engineers, Part B: Journal of Engineering Manufacture*, vol. 216, pp. 697-712, 2002.